Molecular Biology of the Cell
Vol. 11, 1645–1655, May 2000

High-Resolution FRET Microscopy of Cholera Toxin B-Subunit and GPI-anchored Proteins in Cell Plasma Membranes

Anne K. Kenworthy,*† Nadezda Petranova,*‡ and Michael Edidin*

*Department of Biology, The Johns Hopkins University, Baltimore, Maryland 21218; and ‡Laboratory of Leucocytes Antigens, Institute of Molecular Genetics, Academy of Sciences of the Czech Republic, Videnská 1083, 14220 Prague, Czech Republic

Submitted September 10, 1999; Revised January 18, 2000; Accepted March 8, 2000
Monitoring Editor: Guido Guidotti

"Lipid rafts" enriched in glycosphingolipids (GSL), GPI-anchored proteins, and cholesterol have been proposed as functional microdomains in cell membranes. However, evidence supporting their existence has been indirect and controversial. In the past year, two studies used fluorescence resonance energy transfer (FRET) microscopy to probe for the presence of lipid rafts; rafts here would be defined as membrane domains containing clustered GPI-anchored proteins at the cell surface. The results of these studies, each based on a single protein, gave conflicting views of rafts. To address the source of this discrepancy, we have now used FRET to study three different GPI-anchored proteins and a GSL endogenous to several different cell types. FRET was detected between molecules of the GSL GM1 labeled with cholera toxin B-subunit and between antibody-labeled GPI-anchored proteins, showing these raft markers are in submicrometer proximity in the plasma membrane. However, in most cases FRET correlated with the surface density of the lipid raft marker, a result inconsistent with significant clustering in microdomains. We conclude that in the plasma membrane, lipid rafts either exist only as transiently stabilized structures or, if stable, comprise at most a minor fraction of the cell surface.

INTRODUCTION

"Lipid rafts" enriched in glycosphingolipids (GSL) and cholesterol are conceived as spatially differentiated microdomains in cell membranes (Harder and Simons, 1997; Simons and Ikonen, 1997). By preferentially including some proteins and excluding others, lipid rafts and related membrane microdomains such as caveolae may regulate the sorting and trafficking of certain plasma membrane proteins and lipids and compartmentalize cell-signaling events (Verkade and Simons, 1997; Anderson, 1998; Brown and London, 1998; Horejsi *et al.*, 1999). Although lipid rafts have been inferred from functional and kinetic studies of intact cells (Mays *et al.*, 1995; Hannan and Edidin, 1996; Sheets *et al.*, 1997; Keller and Simons, 1998), most evidence of their existence is based on differential extraction of cells with detergent (Skibbens *et al.*, 1989; Stefanova *et al.*, 1991; Brown and Rose, 1992; Fiedler *et al.*, 1993; Sargiacomo *et al.*, 1993). These studies indicate that in addition to GSL and cholesterol, lipid rafts are enriched in GPI-anchored proteins, some transmembrane proteins, and diacylated cytoplasmic proteins including Src family kinases.

The relationship between membrane extracts and the in vivo composition and structure of lipid rafts is uncertain and controversial (Kurzchalia *et al.*, 1995; Edidin, 1997; Harder and Simons, 1997; Simons and Ikonen, 1997; Weimbs *et al.*, 1997; Brown and London, 1998; Hooper, 1998; Jacobson and Dietrich, 1999). One might expect that lipid rafts would concentrate molecules such as GPI-anchored proteins, effectively clustering them. Such domains containing clustered GPI-anchored proteins can sometimes be detected by conventional light or electron microscopy (Matsuura *et al.* 1984; Latker *et al.* 1987; Kobayashi and Robinson, 1991; van den Berg *et al.*, 1995) (reviewed in Anderson [1998]). In other cases clusters of GPI-anchored proteins or other lipid raft components are only apparent when they have been cross-linked with secondary antibodies (Howell *et al.* 1987; Rothberg *et al.*, 1990; Fra *et al.*, 1994; Mayor *et al.*, 1994; Parton *et al.*, 1994; Fujimoto, 1996; Harder *et al.*, 1998). This suggests

† Corresponding author and present address: Cell Biology and Metabolism Branch, National Institute of Child Health and Human Development, National Institutes of Health, Building 18 T, Room 101, Bethesda, MD 20892. E-mail address: kenworta@mail.nih.gov.

Abbreviations used: CTXB, cholera toxin B-subunit; D:A, ratio of donor- to acceptor-labeled probes; E, energy transfer efficiency; FRET, fluorescence resonance energy transfer; GSL, glycosphingolipids; MDCK, Madin–Darby canine kidney; NRK, normal rat kidney; roi, region of interest; 5′ NT, 5′ nucleotidase.

that in vivo, lipid rafts may be small or dynamic structures that are aggregated and stabilized by detergent extraction or by antibody-induced cross-linking (Edidin, 1997; Harder and Simons, 1997; Simons and Ikonen, 1997; Weimbs *et al.*, 1997; Brown and London, 1998; Jacobson and Dietrich, 1999).

Fluorescence resonance energy transfer (FRET) microscopy, a method with a resolution of tens of angstroms, can, in principle, detect lipid rafts defined as membrane domains containing clustered lipid raft components in situ. Yet, two recent studies using FRET microscopy reached opposite conclusions about the existence of rafts in cell membranes. Measuring FRET between donor- and acceptor-labeled antibodies, we found that most molecules of a GPI-anchored protein, 5′ nucleotidase (5′ NT), are randomly distributed at the apical membrane of polarized Madin–Darby canine kidney (MDCK) cells (Kenworthy and Edidin, 1998). This implies either that the entire apical membrane is a single raft or that lipid rafts are vanishingly small, consisting at most of a few GPI-anchored proteins and associated lipids. Another group used a different method to detect FRET between fluorescent folate analogues bound to a GPI-anchored folate receptor. Their results suggest that all molecules of this receptor are clustered in microdomains of ~70 nm in diameter in Chinese hamster ovary and CaCo-2 cells (Varma and Mayor, 1998).

This difference in results may be attributable to technical differences such as the nature of the probes or may reflect biologically relevant variations in the structure and composition of lipid rafts. To address these issues, we have used FRET microscopy to compare the organization of three endogenous GPI-anchored proteins (folate receptor, CD59, and 5′ NT) and a GSL component of lipid rafts, detected using cholera toxin B-subunit (CTXB), in the plasma membrane of several different cell types. The data are not consistent with the concentration of most GPI-anchored proteins and GSL in lipid rafts or with the existence of relatively large (hundreds of nanometers in diameter), stable rafts. They are consistent with a small fraction of marker molecules resident in small and unstable rafts in intact membranes and with a limited capacity of rafts for GSL and GPI-anchored proteins.

MATERIALS AND METHODS

Cells and Antibodies

HeLa cells (HeLa Tet-on cells; Clontech Laboratories, Palo Alto, CA) and normal rat kidney (NRK) cells were maintained in DMEM supplemented with 10% FCS at 37°C in 5% CO_2. Fao cells were maintained in modified Ham's F-12 medium supplemented with 5% FCS at 37°C in 7% CO_2.

Monoclonal antibodies directed against rat 5′ NT (5NT42) (Siddle *et al.*, 1981), rat CD59 (6D1 and TH9) (Hughes *et al.*, 1992), human CD59 (MEM43) (Stefanova *et al.*, 1989), and human folate receptor (MOv19 and MOv18) (Coney *et al.*, 1991) were graciously provided by Dr. J. P. Luzio (University of Cambridge, Cambridge, UK), Dr. B. P. Morgan (University of Wales College of Medicine, Heath Park, Cardiff, UK), Dr. V. Horejsi (Czech Academy of Sciences, Prague, Czech Republic), and Dr. J. Ghrayeb (Centorcor, Malvern, PA), respectively. CTXB was purchased from Sigma Chemical (St. Louis, MO). Cy3- and Cy5-CTXB and IgG conjugates were prepared from succinimidyl ester derivatives according to the manufacturer's instructions (Fluorolink Reactive Dye; Amersham, Arlington Heights, IL). The Cy3- and Cy5-probes bound equally well and specifically; a plot of the binding of the donor-labeled probe versus the binding of the acceptor-labeled probe was highly correlated (typically $R > 0.95$). Binding of either labeled probe was eliminated in the presence of excess unlabeled probe, and no binding was observed on cells that did not express the molecule of interest (our unpublished results).

Preparation of Cells for FRET Microscopy

Labeling and mounting procedures were performed as described previously (Kenworthy and Edidin, 1998, 1999). In all experiments, the concentration of the donor-labeled probe was held constant (10 μg/ml CTXB or 50 μg/ml for antibodies), and the concentration of the acceptor-labeled probe was varied to achieve the indicated donor-to-acceptor ratio (D:A). The antibody/CTXB mixtures were freshly diluted from stock solutions (typically 0.5–1 mg/ml) into phosphate-buffered saline or HEPES-buffered HBSS containing 1% BSA and centrifuged just before use to eliminate large aggregates. Cells grown on coverslips were labeled with the antibody/CTXB mixtures at 4°C for 15 min, washed several times, and then fixed in freshly prepared 4% paraformaldehyde for 30 min at room temperature. For positive controls for clustering, cells were labeled with 50 μg/ml donor-labeled primary antibody followed by an acceptor-labeled secondary antibody at 10 μg/ml before fixation. For control experiments using live cells, the fixation step was omitted. The coverslips were mounted in phosphate-buffered saline or HEPES-buffered HBSS and then sealed with nail polish. Tape spacers were used to separate the coverslips slightly from the slide to increase the volume of mounting solution and to prevent damage to the cells.

FRET Microscopy Measurements

Fluorescence microscopy and the FRET measurements were performed as described previously (Kenworthy and Edidin, 1998, 1999) with minor revisions. Cells were imaged on a Zeiss Axiovert 135TV (Carl Zeiss, Thornwood, NY) using a 1.4 numerical aperture 63× Zeiss Plan-apochromat objective or a 1.3 numerical aperture 100× Zeiss Plan-neofluor objective, and digital images were collected on a 12-bit series 200 cooled charge-coupled device camera (Photometrics, Tuscon, AZ) operated using the IC300 integrated digital-imaging system (Inovision, Research Triangle Park, NC). Cy3 and Cy5 fluorescence was excited using a 75-W xenon arc lamp and detected using appropriate filter sets (Chroma Technology, Brattleboro, VT).

R_o is ~50 Å for Cy3 (donor) and Cy5 (acceptor) (Bastiaens and Jovin, 1996), so FRET will only occur when Cy3- and Cy5-labeled molecules are separated by > ~100 Å (energy transfer efficiency [E] = 1.5% at a 100-Å separation). To measure FRET, we quantitated the quenching of donor fluorescence due in the presence of the energy transfer acceptor. Cells were double labeled with Cy3- and Cy5-conjugated probes at the desired molar (D:A) ratio as described above. An image of Cy3 fluorescence in the presence of the acceptor was collected ($Cy3_{pre}$), followed by an image of Cy5 fluorescence ($Cy5_{pre}$). Cy5 was then irreversibly photobleached by continuous excitation (typically requiring 1–2 min), and an image of the residual Cy5 signal ($Cy5_{post}$) was collected to ensure that complete photobleaching had occurred. This photobleaching step eliminates Cy5 as an energy transfer acceptor. A final image of the Cy3 fluorescence was then obtained ($Cy3_{post}$). After subtracting the dark-current contribution from each image, the fluorescence intensity from identical regions of interest (rois) on individual cells was tabulated for each of these images ($Cy3_{pre}$, $Cy5_{pre}$, $Cy5_{post}$, and $Cy3_{post}$) using a custom-written macro. The E of each roi was then calculated as follows: $E\,(\%) = 100 \times (Cy3_{post} - Cy3_{pre})/Cy3_{post}$. This differs slightly from our previous method (Kenworthy and Edidin, 1998) in which E was determined from a calculated E image. We have now found that calculating E from the mean fluorescence intensities of rois sampled on the $Cy3_{pre}$ and $Cy3_{post}$ images is more accurate in the limit of low E, because it allows E to be < 0 (see Figures 3 and 4 for the results of donor-only–labeled controls). In the calculated E images, E is constrained to be > 0.

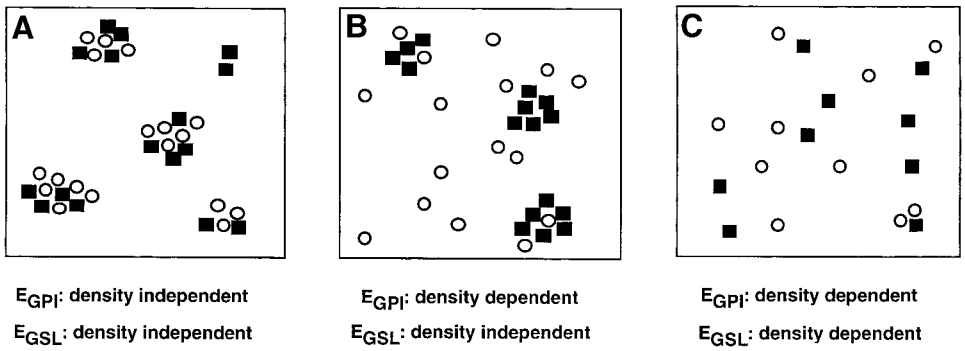

Figure 1. Models for the organization of GSL and GPI-anchored proteins in lipid rafts at the cell surface. ■, GSL; ○, GPI-anchored proteins. (A) Coclustering model. Lipid rafts are microdomains large enough to contain tens to hundreds of GSL and GPI-anchored proteins. They may be stabilized by specific proteins such as caveolin. (B) Differential clustering model. Proteins and lipids associate with rafts to extents that depend on their affinities for lipid microdomains of a given composition and physical state. In both A and B, the total protein or GSL content of the membrane could affect E between labeled components of the rafts. High levels of GSL might enhance clustering of GPI-anchored proteins in lipid rafts. Alternatively, GPI-anchored proteins, and perhaps GSL, may compete for limited amounts of raft-forming lipids such as cholesterol. (C) Unstable or very small raft model. Mobile lipids and proteins found in biochemically isolated lipid raft fractions are normally dispersed at random, although their interaction with lipids may show some specificity. Cross-linking or other perturbations aggregate the complexes and stabilize them. Variations of these models have been described previously (Harder and Simons, 1997; Simons and Ikonen, 1997; Brown and London, 1998; Jacobson and Dietrich, 1999). See the text for details of how FRET microscopy measurements can discriminate between these models.

Each set of FRET data shown is from a single experiment and is representative of two or more independent experiments. In a typical experiment, four to five fields of cells were measured for each sample. Occasionally data from a single field were systematically different from that from the other fields measured for the same sample. This effect is likely caused by local variations in the environment that affect overall fluorescence quenching. These outlier data were not included in the final analysis, because their inclusion would have distorted the "baseline" fluorescence intensity. This in turn could alter the apparent value of E, which is normalized to this baseline for all of the cells in that field. In control experiments using live cells, only one to two fields could be measured, because after a short period of time Cy5 fluorescence could no longer be photobleached. This is presumably because of oxygen depletion from the medium. Acceptor fluorescence intensities (presented here in arbitrary units) were normalized for exposure time within an experiment to allow for comparison of the different D:A ratios. No corrections were made for the dye:protein ratio of the different markers (this ranged between 1 and 3). The acceptor fluorescence is not directly comparable between experiments unless specifically indicated, because imaging conditions were optimized for each experiment.

RESULTS

Rationale for Using FRET Microscopy to Detect Lipid Rafts

FRET microscopy detects the proximity of appropriately labeled or intrinsically fluorescent lipids and proteins with a resolution of tens of angstroms (Uster and Pagano, 1986; Herman, 1989; Jovin and Arndt-Jovin, 1989; Tsien *et al.*, 1993; Nagy *et al.*, 1998; Ng *et al.*, 1999; Pollok and Heim, 1999). The efficiency of energy transfer E for a donor and acceptor fluorophore separated by distance r is given by the following: $E = 1/\{1 + (r/R_o)^6\}$, where R_o is a characteristic of the donor and acceptor pair and is typically 30–60 Å. Considering molecules in the plasma membrane, we can see that for a given surface concentration, some fraction of a population of randomly distributed molecules may be within FRET distance of one another by chance. On the other hand, molecules concentrated in microdomains, at a higher concentration than average for the entire membrane, will have a higher chance of being within FRET distance than will those randomly distributed (Kenworthy and Edidin, 1998) (Figure 1). These cases can be distinguished experimentally using three criteria based on theoretical predictions for FRET between donors and acceptors in membranes (summarized in Kenworthy and Edidin [1998]). For randomly distributed molecules (Figure 1C), E should 1) increase as a function of acceptor surface density, 2) go to zero in the limit of low acceptor surface densities, and 3) be independent of the molar ratio of donor- to acceptor-labeled molecules D:A. For clustered molecules (Figure 1A), E should be completely independent of the surface density and should depend on D:A. For mixtures of randomly distributed and clustered molecules, the experimental data should be intermediate between that predicted for a purely random and a purely clustered distribution. We have estimated previously that the lower limit of detection of our method is ~20% clustered, with 80% randomly distributed (Kenworthy and Edidin, 1998).

Plasma Membrane Distribution of Lipid Raft Markers Detected by Fluorescence Microscopy

As a marker for the GSL components of lipid rafts, we used CTXB, which specifically binds the ganglioside GM1. CTXB is enriched in biochemical lipid raft fractions and in caveolae (Fra *et al.*, 1994; Parton *et al.*, 1994; Parton, 1996; Smart *et al.*, 1995; Schnitzer *et al.*, 1996; Harder and Simons, 1997; Stauffer and Meyer, 1997; Henley *et al.*, 1998; Orlandi and Fishman, 1998; Wolf *et al.*, 1998; Lencer *et al.*, 1999). Three GPI-anchored proteins, which are major components of detergent-insoluble raft fractions (Skibbens *et al.*, 1989; Stefanova *et al.*, 1991; Brown and Rose, 1992; Fiedler *et al.*, 1993; Sargiacomo *et al.*, 1993), were used as protein markers for lipid rafts. These include CD59, an inhibitor of complement-mediated cell lysis (Walsh *et al.*, 1992); 5′ NT (CD73), an ectoenzyme (Zimmermann, 1992); and folate receptor, which binds and internalizes folic acid (Antony, 1992).

By fluorescence microscopy, endogenous GM1 and GPI-anchored proteins appeared diffusely distributed across the

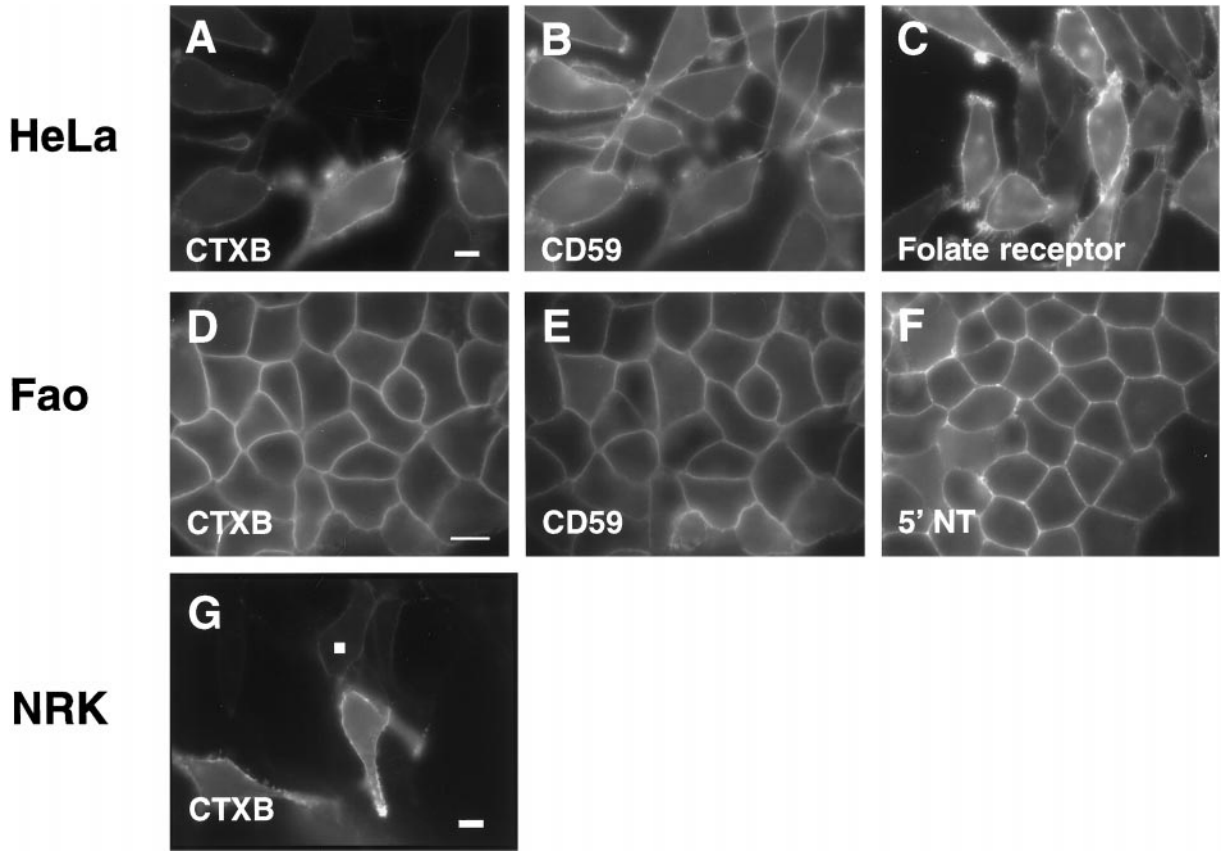

Figure 2. Cell surface expression of GM1 and of endogenous GPI-anchored proteins visualized by fluorescence microscopy. GM1 was detected with Cy3- or Cy5-labeled CTXB (A, D, and G), and labeled monoclonal antibodies were used to detect human CD59 (B), human folate receptor (C), rat CD59 (E), or rat 5′ NT (F) in HeLa (A–C), Fao (D–F), and NRK (G) cells. Exposure times were optimized to maximize the signal for each marker, so their relative fluorescence intensities are not directly comparable. Note however that the levels of surface expression varied significantly from cell to cell for some of the markers (A, C, and G) and that the expression of the various markers was not correlated in double-labeled cells (compare A with B and D with E). The white box in G corresponds to a typical roi sampled to obtain the data presented below (see Figures 3–6) for NRK and HeLa cells. For Fao cells, smaller rois centered on the lines of plasma membrane label were used (not visible in this figure). Bars: A—C, D—F, and G, 10 μm.

plasma membranes of three morphologically unpolarized cell types, HeLa, NRK, and Fao, when these were labeled directly using fluorescently tagged CTXB or monoclonal antibodies (IgG) (Figure 2). At the resolution of the light microscope, no obvious enrichment of CTXB or GPI-anchored proteins in distinct microdomains could be seen (Figure 2). If cells were instead labeled with monoclonal antibodies followed by anti-mouse Ig and briefly incubated at 37°C before fixation, discrete spots of label were seen (our unpublished results). These puncta were similar to those reported in previous studies (Rothberg *et al.*, 1990; Mayor *et al.*, 1994; Fujimoto, 1996; Harder *et al.*, 1998; Kenworthy and Edidin, 1998). The plasma membrane distribution of CTXB and GPI-anchored proteins was more diffuse and extensive than that of caveolin-1 or -2, which could be detected by indirect immunofluorescence microscopy in HeLa and NRK cells but not in Fao cells (our unpublished results). That neither the GPI-anchored proteins nor CTXB appear to be exclusively associated with caveolin/caveolae is in agreement with previous reports (Montesano *et al.*, 1982; Mayor *et al.*, 1994; Parton, 1994; Fujimoto, 1996). Because clustering of CTXB in caveolae in living cells is enhanced with increasing the temperature of incubation (Parton, 1994), in our experiments cells were labeled on ice, a condition in which minimal clustering occurs, and then immediately fixed.

CTXB and all of the GPI-anchored proteins studied here have been identified previously as components of lipid rafts defined biochemically (van den Berg *et al.*, 1995; Smart *et al.*, 1996; Strohmeier *et al.*, 1997; Hatanaka *et al.*, 1998). We confirmed this in HeLa cells by incubating labeled cells in PBS containing 1% Triton X-100 for 30 min on ice and then fixing the cells and visualizing the detergent-insoluble membrane fraction by fluorescence microscopy (Mayor and Maxfield, 1995; Kenworthy and Edidin, 1998). As expected, CTXB, folate receptor, and CD59 all were present after detergent extraction at levels similar to that of mock-extracted cells, whereas transferrin receptor labeled with fluorescently tagged human transferrin was completely extracted under these conditions (our unpublished results).

FRET Microscopy Measurements of CTXB, a Marker for GSL in Lipid Rafts

To perform FRET measurements, we labeled living cells at 4°C with Cy3- and Cy5-tagged CTXB or antibodies and then fixed the cells before imaging to capture a snapshot of domain organization. FRET was quantitated as the release of donor quenching after irreversibly photobleaching the acceptor (Bastiaens and Jovin, 1996; Kenworthy and Edidin, 1998, 1999). We then examined the dependence of the energy transfer efficiency E on the fluorescence intensity of the bound probes (which is proportional to their surface density) on a cell-by-cell basis.

FRET between donor- and acceptor-labeled CTXB was found to correlate with the surface density of bound CTXB in NRK and HeLa cells and went to zero in the limit of very low acceptor surface densities (Figure 3, A and B). These observations, combined with the dependence of E on surface density, exclude the possibility that all the bound CTXB is clustered (Figure 1) and indicate instead that CTXB is randomly distributed or alternatively that only a fraction of CTXB is clustered. These alternatives were distinguished by testing the dependence of E on D:A. If a fraction of these molecules is clustered, then E should vary as a function of the molar fraction of donor- and acceptor-labeled molecules. In HeLa and NRK cells, E was independent of this ratio over the range 1:1–1:3 (Figure 3, A and B). This result suggests that most CTXB is randomly distributed under the conditions of these experiments.

In Fao cells, CTXB bound at surface densities that were at least 10-fold higher than that in HeLa and NRK cells (Figure 3C). A correspondingly high value of E was measured, and this E showed little cell-to-cell dependence. This could indicate that either all or some fraction of CTXB is clustered in Fao cells. Because endogenous GM1 levels were uniformly high across the Fao cell population, we could not directly confirm whether E went to zero in the limit of low surface densities of bound CTXB. Nevertheless these data provide a useful comparison with other raft markers in these cells (see below), as well as with the behavior of CTXB in the other cell types (Figure 3C).

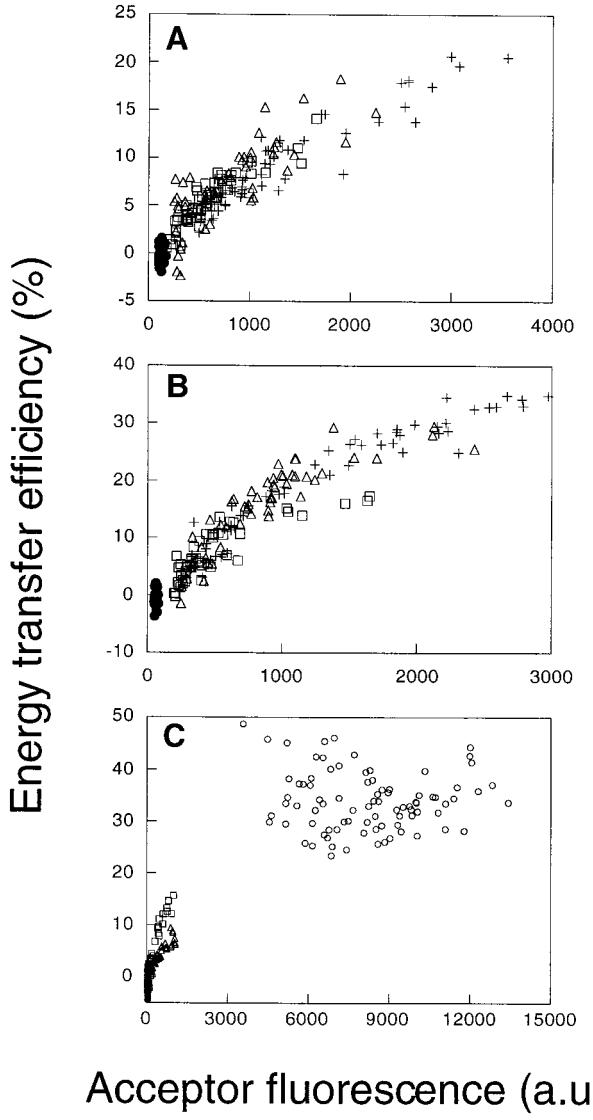

Figure 3. Energy transfer efficiencies between donor- and acceptor-labeled CTXB are dependent on their surface density in the plasma membrane of several cell types. (A and B) E measured between labeled CTXB in HeLa (A) and NRK (B) cells for D:A ratios of 1:1 (□), 1:2 (△), and 1:3 (+). Control samples were labeled with Cy3-labeled CTXB only (●). Each data point in these plots is taken from a single cell, sampled from an roi as defined in Figure 2. Note that in this figure the absolute fluorescence intensities in A and B are comparable. (C) Comparison of FRET for CTXB in HeLa (△), NRK (□), and Fao (○) cells. The mean E for CTXB in Fao cells ranged from 20 to 40% (n = 7 independent experiments) but was always significantly higher than that measured in NRK or HeLa cells in the same experiment. a.u., arbitrary units.

FRET Microscopy Measurements for GPI-anchored Proteins

Using donor- and acceptor-labeled antibodies as probes, we measured FRET for the GPI-anchored folate receptor. Previously FRET anisotropy measurements of this molecule labeled with a fluorescent folate analogue were interpreted as showing that all molecules of this protein were in lipid rafts (Varma and Mayor, 1998). We found that E between folate receptors labeled with the monoclonal antibody MOv19 depended on the surface density of the label in HeLa cells and went to zero for cells with low folate receptor surface densities (Figure 4). These data contrast with the density-independent E reported for folate receptor labeled with a fluorescent folate analogue (Varma and Mayor, 1998) and exclude the possibility that all molecules of the folate receptor are clustered in rafts in our cells. E for the folate receptor was independent of D:A over a range of 1:1–1:3 (Figure 4). This also suggests that most folate receptor is randomly distributed.

We considered the possibility that binding of antibody may disperse preexisting clusters of folate receptor. Binding of MOv19 has been shown to disrupt biochemically defined clusters of folate receptor in situ (Smart *et al.*, 1996). We therefore also measured FRET using another anti-folate receptor antibody, MOv18, that does not disrupt such clusters

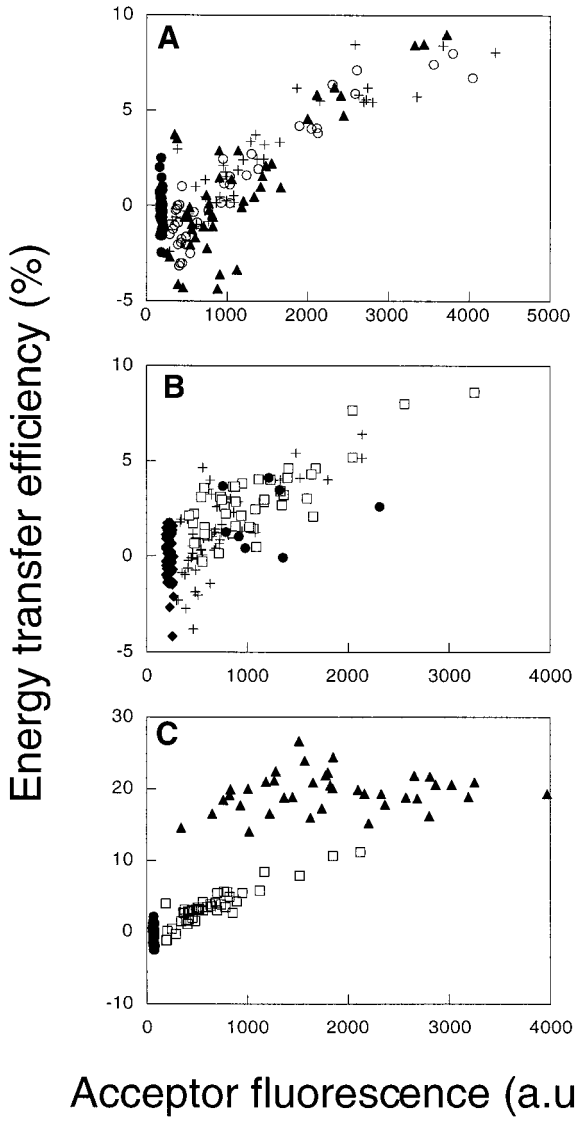

Figure 4. Energy transfer efficiencies between donor- and acceptor-labeled anti-folate receptor antibodies are dependent on their density in HeLa cell plasma membranes. (A) E measured between the labeled anti-folate receptor IgG MOv19 for D:A ratios of 1:1 (○), 1:2 (+), and 1:3 (▲). Control samples were labeled with Cy3-labeled probe only (●). (B) E measured between the labeled anti-folate receptor IgG MOv19 (□) and MOv18 (+) at a D:A of 1:1. Control samples include fixed cells labeled with Cy3-MOv18 only (♦) and live cells labeled with MOv18 at a D:A of 1:1 (●). (C) A positive control demonstrating the detection of clustering between directly bound molecules. E measured between Cy3- and Cy5-labeled MOv19 (□) is density dependent, whereas E between Cy3-labeled MOv19 and Cy5 donkey anti-mouse IgG (▲) is independent of surface density and is significant (E ~ 20%) even at low acceptor surface densities. Negative control samples were labeled with Cy3-labeled probe only (●).

(Smart *et al.*, 1996). FRET measurements for MOv18 and MOv19 yielded very similar results, both showing the density-dependent energy transfer characteristic of randomly distributed molecules in HeLa (Figure 4B) and CaCo-2 cells (our unpublished results). Because clustering of folate receptor was not detected even with MOv18, our FRET microscopy measurements appear to be sensitive to properties of the membrane environment of the folate receptor different from those reported by the detergent-free cell fractionation method (Smart *et al.*, 1996).

Certain fixation conditions have been shown recently to disrupt clusters of folate receptor detected by electron microscopy (Wu *et al.*, 1997). To address the possibility that our results are caused by such dispersion, in control experiments we measured FRET between antibody-labeled folate receptors in living cells. If clustered folate receptors disperse after fixation, then we would expect to obtain a higher E in live cells than in fixed cells, particularly at low acceptor densities. Instead, we observed similar values of E for folate receptor labeled with MOv18 in live and fixed cells (Figure 4B), suggesting that our fixation conditions do not significantly alter the organization of folate receptor in the membrane.

To confirm that we could detect clustered molecules using this assay, we measured FRET on HeLa cells labeled with Cy3-labeled MOv19 followed by Cy5 donkey anti-mouse Ig. As we described previously (Kenworthy and Edidin, 1998), this is a positive control for "clustering" because all the acceptor-labeled molecules must be directly bound to donor-labeled molecules. As predicted by theoretical models for clustered molecules (Kenworthy and Edidin, 1998), this gave rise to density-independent E, and there was significant E even in the limit of very low acceptor surface densities (Figure 4C). Moreover, at any given surface density the magnitude of E was higher than that observed between the donor- and acceptor-labeled MOv19 in the same experiment (Figure 4C).

We next measured FRET for two additional GPI-anchored proteins. FRET measurements for CD59 yielded E values close to zero in both HeLa (Figure 5A) and Fao cells (Figure 5B). Such low values of E are inconsistent with a clustered distribution for CD59. They would be expected however for a random distribution (Figure 1C) because of the relatively low surface density of CD59 in these cells. Although CD59 has been reported recently to be a dimer (Hatanaka *et al.*, 1998), such dimers are not detected in our experiments. FRET measurements for a third GPI-anchored protein, 5′ NT, the protein we studied previously in MDCK cells (Kenworthy and Edidin, 1998), yielded slightly higher values of E than did measurements for CD59 in Fao cells (Figure 5B). These values are similar to, but slightly higher than, the predicted E of ~1% we calculated from theoretical equations (Wolber and Hudson, 1979; Dewey and Hammes, 1980) assuming r = 0 and a surface density of ~100 monomers of 5′ NT/μm^2 at the Fao cell plasma membrane (Howell *et al.*, 1987). 5′ NT exhibited a relatively weak cell-to-cell dependence of E on surface density, but similar curves were obtained for D:A of 1:1–1:3 (our unpublished results).

FRET between a GPI-anchored Protein and CTXB

If most CTXB and most GPI-anchored proteins are randomly distributed with respect to one another in a given cell, then FRET between CTXB and a GPI-anchored protein should also be consistent with a random distribution; i.e., E should be density dependent and go to zero in the limit of low acceptor densities and should show no dependence on D:A.

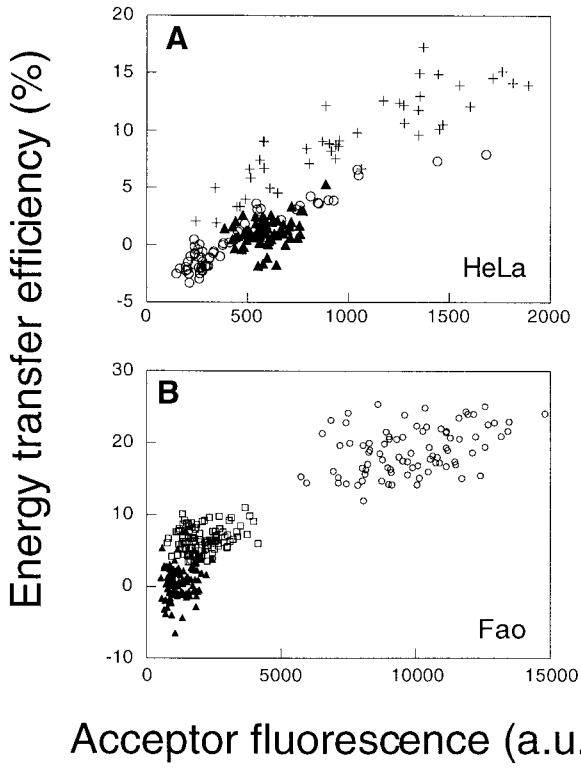

Figure 5. Energy transfer efficiencies correlate with the surface densities of endogenous GPI-anchored proteins and CTXB in HeLa and Fao cells. (A) Comparison of E for CTXB (+), CD59 (▲), and folate receptor (○) in HeLa cells. (B) Comparison of E for CTXB (○), 5′ NT (□), and CD59 (▲) in Fao cells.

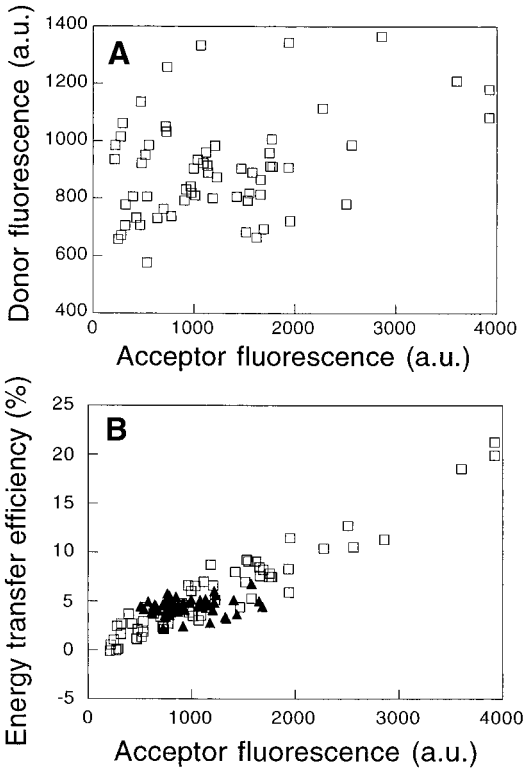

Figure 6. Energy transfer between a GPI-anchored protein and a GSL is consistent with their being randomly distributed with respect to one another. (A) Plot demonstrating the lack of correlation between the surface expression of CD59 and CTXB binding in individual HeLa cells. Each symbol shows the fluorescence intensity of Cy3-anti-CD59 IgG and Cy5-CTXB for a single cell. (B) FRET measured between Cy3-anti-CD59 IgG and Cy5-CTXB (□) or Cy3-CTXB and Cy5-anti-CD59 IgG (▲) in HeLa cells. Because of the cell-to-cell variation in the surface densities of CTXB and CD59 on individual HeLa cells (A), D:A varied >15-fold in this experiment.

We tested this prediction in HeLa cells, in which the surface densities of the various lipid raft markers varied independently (Figures 2 and 6A). In these experiments, E correlated with the surface density of the acceptor-labeled probe and was independent of D:A over a 15-fold range (Figure 6B). Note that the range of acceptor surface densities is smaller when CD59 is the acceptor-labeled molecule than when CTXB is the acceptor, as demonstrated above (Figure 5A).

In addition to providing independent verification that most molecules of our raft markers are distributed randomly with respect to both themselves and one another, these data also show that the distribution of raft markers is independent of their relative concentrations in the membrane. For example, the organization of CD59 appears to be similar in cells containing either high or low amounts of GM1 at the cell surface, because identical, low values of E are obtained in each case (Figure 6). Even though the protein or GSL content of the membrane could presumably affect E between labeled components of rafts by competing for or dispersing clusters (Figure 1), such effects are not apparent in our experiments.

DISCUSSION

One of the simplest predictions of the lipid raft hypothesis is that proteins and lipids of rafts are concentrated or clustered relative to their average concentration in the cell surface membrane. FRET microscopy, which measures molecular proximity on a scale of < 100 Å, might be expected to detect such clusters unambiguously. Yet, even this approach has provided conflicting evidence of the existence of rafts (Kenworthy and Edidin, 1998; Varma and Mayor, 1998). This was especially surprising because even though one study used donor quenching to measure energy transfer and the other used fluorescence anisotropy, each study used a similar criterion to detect clustering of lipid raft components by evaluating the dependence of E on surface density across a population of cells expressing a differing amount of protein. The difference in outcome of the two studies could be technical, or could be attributable to biology, because two different proteins were examined and different cell types were used. To address the difference we used our FRET microscopy technique to study four different molecules associated with lipid rafts, in three different cell types.

We measured FRET for CTXB, a marker for GSL in lipid rafts, as well as three GPI-anchored proteins detected with labeled antibodies: folate receptor, CD59, and 5′ NT. By biochemical criteria, each of these molecules has been found

previously to be associated with lipid rafts. Our FRET results are not consistent with the idea that most or all molecules of each of these molecules are concentrated in lipid rafts in intact cell membranes. Rather, FRET was consistent with the idea that most molecules of each marker are randomly distributed in the cell plasma membrane. For some markers this was evidenced by increasing FRET efficiency with increasing surface concentration of fluorescent acceptor. For other markers this was evidenced by low absolute values of FRET. For example, for CD59, E was essentially zero in two different cell types, a result inconsistent with clustering (Figure 5). Furthermore, the magnitude of E varied for different lipid raft markers. For example, CTXB gave systematically higher E values than did antibody-labeled GPI-anchored proteins when compared at the same acceptor fluorescence intensity (Figure 5B). Such behavior is predicted for randomly distributed molecules of different sizes or geometries (Wolber and Hudson, 1979; Dewey and Hammes, 1980). These findings provide evidence that the FRET results are specific and that we should be able to detect clustered membrane proteins.

Our results are inconsistent with the idea that the organization of lipid raft components differs in the plasma membrane of polarized and nonpolarized cells. We suggested previously that 5′ NT might appear to be randomly distributed in the apical membrane of polarized MDCK cells because the entire apical membrane is a single raft (Kenworthy and Edidin, 1998). In contrast, if the plasma membrane of nonpolarized cells such as those examined by Varma and Mayor (1998) was a mixture of raft and nonraft domains, this could explain why folate receptor appeared to be clustered there. Such domains could potentially originate from raft-based sorting mechanisms in the secretory pathway, which are thought to be similar in polarized and nonpolarized cells (reviewed in Keller and Simons [1997]; Verkade and Simons [1997]; Brown and London [1998]). However, in the current study, we did not find evidence of significant clustering of either GPI-anchored proteins or CTXB in the plasma membrane of several different morphologically unpolarized cell types (Figures 3–6). If a mixture of raft and nonraft domains exists in the plasma membrane of these cells, it is not readily detected in our experiments. The distribution of both GPI-anchored proteins and CTXB also appears to be independent of caveolin/caveolae. This is consistent with the finding that GPI-anchored proteins are not enriched in caveolae unless they are cross-linked with antibodies (Mayor *et al*., 1994; Fujimoto, 1996) and that CTXB labeling is not confined exclusively to caveolae (Montesano *et al*., 1982; Parton, 1994). In fact, the highest E we observed was for CTXB in Fao cells (Figures 3C and 5B), in which no caveolin labeling could be detected by immunofluorescence microscopy (our unpublished results).

It has been suggested that lipid rafts may be disrupted by antibody binding (Anderson, 1998; Jacobson and Dietrich, 1999; Kurzchalia and Parton, 1999). However, most data indicate that antibody binding and cross-linking do not disrupt (our unpublished results) (Mayor and Maxfield, 1995; Kenworthy and Edidin, 1998) and indeed may stabilize (Harder *et al*., 1998) the association of proteins with lipid rafts. The great exception is the observation that clustering of folate receptor is disrupted by binding of the antibody MOv19 (Smart *et al*., 1996). This effect is epitope specific because a second antibody, MOv18, did not disrupt folate receptor clusters. We measured FRET between folate receptors labeled with each of these two antibodies and found that both reported a random distribution of folate receptor. It is formally possible that the distribution of GPI-anchored folate receptor changes from random to clustered in response to folate binding. However our cells were cultured in medium containing folic acid. Hence this cannot explain why clustering of the folate receptor is observed when detected using a fluorescent folate analogue (Varma and Mayor, 1998) but not in our experiments using antibody probes. We also found that another lipid raft component, GM1, detected using CTXB rather than antibody binding as a probe, gave results consistent with a random distribution in several cell types. Rather than disperse rafts, CTXB binding should act to stabilize the association of GM1 with lipid rafts, because it increases the detergent insolubility of GM1 (Hagmann and Fishman, 1982) and causes enrichment of GM1 in caveolae (Parton, 1994). Taken together these results suggest that antibody binding does not disperse clustered components of lipid rafts.

It has also been suggested that fixation destabilizes lipid rafts or fails to preserve their native structure (Anderson, 1998; Jacobson and Dietrich, 1999; Kurzchalia and Parton, 1999). Recent data indicate that some fixation conditions can disperse clustered folate receptors, detected by electron microscopy (Wu *et al*., 1997). However, our results comparing FRET in fixed cells with that in living cells show that our fixation conditions do not significantly alter the distribution of antibody-labeled folate receptor in living cells (Figure 4B).

Although clustering of lipid raft components can be disrupted by altering levels of various raft components (Varma and Mayor, 1998; Simons *et al*., 1999), it seems unlikely that such an effect occurs in our experiments, which were performed using endogenous markers for rafts. We obtained a similar, density-dependent energy transfer for both endogenous (this study) and transfected (Kenworthy and Edidin, 1998) GPI-anchored proteins, indicating that these molecules had not been artificially dispersed from a clustered distribution because of saturation of the available raft lipids or competition for enrichment in a limited number of clusters.

How then can we reconcile the apparently clustered distribution of folate receptor obtained by anisotropy measurements and the apparently random distribution of this protein and other raft markers using our FRET technique? One possible explanation is that lipid rafts are even smaller than 70 nm in diameter and are too small and/or few in number for us to detect. If lipid rafts consisted of only a few GPI-anchored proteins and associated lipids, then our probes could underestimate the extent of clustering if they were large relative to the size of the microdomain, preventing simultaneous binding of probes to adjacent raft components. Such small domains would be sufficient to account for the weak and/or transient clustering of GPI-anchored green fluorescent protein in HeLa cell plasma membranes detected by another proximity-imaging method (De Angelis *et al*., 1998). Because even Fab fragments (Kenworthy and Edidin, 1998) and CTXB report density-dependent energy transfer, lipid rafts must be too small to allow binding of two molecules

of these labels to components of a single raft. Our results for CTXB and 5′ NT in Fao cells are a possible exception to this model (Figures 3C and 5B). Here, E did not show a clear dependence on surface density, which itself varied only modestly for a given marker within the cell population (Figure 2). At this time we cannot conclusively exclude a clustered distribution of 5′ NT and CTXB in Fao cell membranes. However, if clusters are present, they are not large enough to be detected by electron microscopy, because 5′ NT appears dispersed in the plasma membrane of Fao cells unless it is cross-linked (Howell *et al*., 1987).

It is also possible that a small fraction of the raft markers we have examined is clustered in microdomains but the majority is randomly distributed. Model calculations indicate that it may be difficult to distinguish a purely random population from the case in which only a small fraction of the molecules is clustered or in which density-dependent clustering occurs (Kenworthy and Edidin, 1998). Such model calculations also make strong predictions for the conditions under which E would be completely independent of surface density (Blackman *et al*., 1998; Kenworthy and Edidin, 1998), as was observed in FRET anisotropy measurements of folate receptor (Varma and Mayor, 1998). This could occur either if the majority of folate receptors were clustered or if only a small fraction of folate receptors were clustered but the FRET contribution of folate receptors randomly distributed outside clusters was minimal (because of their low concentration). Preliminary calculations suggest that the anisotropy data for folate receptor are in fact consistent with the enrichment of only a small fraction of folate receptors in clusters, with the majority of the molecules being distributed randomly at low densities outside these domains (Mayor, personal communication). This could explain our inability to detect such clusters readily in our measurements. Further work will be required to identify additional conditions under which such clustering can be detected and the physiological relevance of these clustered molecules.

ACKNOWLEDGMENTS

Mrs. Taiyin Wei, Ms. Tsvetalina Penchava, and Mr. Babatomiwa Adegbenro assisted with image processing. We thank Drs. Benjamin Nichols, Jennifer Lippincott-Schwartz, and Joshua Zimmerberg for helpful discussions. The FRET microscopy experiments were performed at the Integrated Microscopy Facility in the Department of Biology at The Johns Hopkins University (Baltimore, MD). This work was supported by National Institutes of Health grant 5PO1 DK-44375 to M.E.

REFERENCES

Anderson, R.G.W. (1998). The caveolae membrane system. Annu. Rev. Biochem. *67*, 199–225.

Antony, A.C. (1992). The biological chemistry of folate receptors. Blood *79*, 2807–2820.

Bastiaens, P.I., and Jovin, T.M. (1996). Microspectroscopic imaging tracks the intracellular processing of a signal transduction protein: fluorescent-labeled protein kinase C beta I. Proc. Natl. Acad. Sci. USA *93*, 8407–8412.

Blackman, S.M., Piston, D.W., and Beth, A.H. (1998). Oligomeric state of human erythrocyte band 3 measured by fluorescence resonance energy homotransfer. Biophys. J. *75*, 1117–1130.

Brown, D.A., and London, E. (1998). Functions of lipid rafts in biological membranes. Annu. Rev. Cell Dev. Biol. *14*, 111–136.

Brown, D.A., and Rose, J.K. (1992). Sorting of GPI-anchored proteins to glycolipid-enriched membrane subdomains during transport to the apical cell surface. Cell *68*, 533–544.

Coney, L.R., Tomassetti, A., Carayannopoulos, L., Frasca, V., Kamen, B.A., Colnaghi, M.I., and Zurawski, V.J. (1991). Cloning of a tumor-associated antigen: MOv18 and MOv19 antibodies recognize a folate-binding protein. Cancer Res. *51*, 6125–6132.

De Angelis, D.A., Miesenbock, G., Zemelman, B.V., and Rothman, J.E. (1998). PRIM: proximity imaging of green fluorescent protein-tagged peptides. Proc. Natl. Acad. Sci. USA *95*, 12312–12316.

Dewey, T.G., and Hammes, G.G. (1980). Calculation of fluorescence resonance energy transfer on surfaces. Biophys. J. *32*, 1023–1035.

Edidin, M. (1997). Lipid microdomains in cell surface membranes. Curr. Opin. Struct. Biol. *7*, 528–532.

Fiedler, K., Kobayashi, T., Kurzchalia, T.V., and Simons, K. (1993). Glycosphingolipid-enriched, detergent-insoluble complexes in protein sorting in epithelial cells. Biochemistry *32*, 6365–6373.

Fra, A.M., Williamson, E., Simons, K., and Parton, R.G. (1994). Detergent-insoluble glycolipid microdomains in lymphocytes in the absence of caveolae. J. Biol. Chem. *269*, 30745–30748.

Fujimoto, T. (1996). GPI-anchored proteins, glycosphingolipids, and sphingomyelin are sequestered to caveolae only after crosslinking. J. Histochem. Cytochem. *44*, 929–941.

Hagmann, J., and Fishman, P.H. (1982). Detergent extraction of cholera toxin and gangliosides from cultured cells and isolated membranes. Biochim. Biophys. Acta *720*, 181–187.

Hannan, L.A., and Edidin, M. (1996). Traffic, polarity, and detergent solubility of a glycosylphosphatidylinositol-anchored protein after LDL-deprivation of MDCK cells. J. Cell Biol. *133*, 1265–1276.

Harder, T., Scheiffele, P., Verkade, P., and Simons, K. (1998). Lipid domain structure of the plasma membrane revealed by patching of membrane components. J. Cell Biol. *141*, 929–942.

Harder, T., and Simons, K. (1997). Caveolae, DIGs, and the dynamics of sphingolipid-cholesterol microdomains. Curr. Opin. Cell Biol. *9*, 534–542.

Hatanaka, M., Seya, T., Miyagawa, S., Matsumoto, M., Hara, T., Tanaka, K., and Shimizu, A. (1998). Cellular distribution of a GPI-anchored complement regulatory protein CD59—homodimerization on the surface of HeLa and CD59-transfected CHO cells. J. Biochem. *123*, 579–586.

Henley, J.R., Krueger, E.W.A., Oswald, B.J., and McNiven, M.A. (1998). Dynamin-mediated internalization of caveolae. J. Cell Biol. *141*, 85–99.

Herman, B. (1989). Resonance energy transfer microscopy. Methods Cell Biol. *30*, 219–243.

Hooper, N.M. (1998). Membrane biology—do glycolipid microdomains really exist. Curr. Biol. *8*, R114–R116.

Horejsi, V., Drbal, K., Cebecauer, M., Cerny, J., Brdicka, T., Angelisova, P., and Stockinger, H. (1999). GPI-microdomains: a role in signaling via immunoreceptors. Immunol. Today *20*, 356–361.

Howell, K.E., Reuter-Carlso, U., Devaney, E., Luzio, J.P., and Fuller, S.D. (1987). One antigen, one gold? A quantitative analysis of immunogold labeling of plasma membrane 5′ nucleotidase in frozen thin sections. Eur. J. Cell Biol. *44*, 318–327.

Hughes, T.R., Piddelsden, S.J., Williams, J.D., Harrison, R.A., and Morgan, B.P. (1992). Isolation and characterization of a membrane protein from rat erythrocytes which inhibits lysis by the membrane attack complex of rat complement. Biochem. J. *284*, 169–176.

Jacobson, K., and Dietrich, C. (1999). Looking at lipid rafts? Trends Cell Biol. *9*, 87–91.

Jovin, T.M., and Arndt-Jovin, D.J. (1989). FRET microscopy: digital imaging of fluorescence resonance energy transfer. Application in cell biology. In: Cell Structure and Function by Microspectrofluorimetry, ed. E. Kohen, J.S. Ploem, and J.G. Hirschberg, Orlando, FL: Academic Press, 99–117.

Keller, P., and Simons, K. (1997). Post-Golgi biosynthetic trafficking. J. Cell Sci. *110*, 3001–3009.

Keller, P., and Simons, K. (1998). Cholesterol is required for surface transport of influenza virus hemagglutinin. J. Cell Biol. *140*, 1357–1367.

Kenworthy, A.K., and Edidin, M. (1998). Distribution of a glycosylphosphatidylinositol-anchored protein at the apical surface of MDCK cells examined at a resolution of < 100 Å using imaging fluorescence resonance energy transfer. J. Cell Biol. *142*, 69–84.

Kenworthy, A.K., and Edidin, M. (1999). Imaging fluorescence resonance energy transfer as a probe of membrane organization and molecular associations of GPI-anchored proteins. In: Protein Lipidation Protocols, vol. 116, ed. M.H. Gelb, Totowa, NJ: Humana Press, 37–49.

Kobayashi, T., and Robinson, J.M. (1991). A novel intracellular compartment with unusual secretory properties in human neutrophils. J. Cell Biol. *113*, 743–756.

Kurzchalia, T.V., Hartmann, E., and Dupree, P. (1995). Guilt by insolubility: does a protein's detergent insolubility reflect a caveolar location? Trends Cell Biol. *5*, 187–189.

Kurzchalia, T.V., and Parton, R.G. (1999). Membrane microdomains and caveolae. Curr. Opin. Cell Biol. *11*, 424–431.

Latker, C., Shinoware, N.L., Miller, J.C., and Rapoport, S.I. (1987). Differential localization of alkaline phosphatase in barrier tissues of the frog and rat nervous system: a cytochemical and biochemical approach. J. Comp. Neurol. *264*, 291–302.

Lencer, W.I., Hirst, T.R., and Holmes, R.K. (1999). Membrane traffic and the cellular uptake of cholera toxin. Biochim. Biophys. Acta *1450*, 177–190.

Matsuura, S., Eto, S., Kato, K., and Tashiro, Y. (1984). Ferritin immunoelectron microscopic localization of 5′ nucleotidase on rat liver cell surface. J. Cell Biol. *99*, 166–173.

Mayor, S., and Maxfield, F.R. (1995). Insolubility and redistribution of GPI-anchored proteins at the cell surface after detergent treatment. Mol. Biol. Cell *6*, 929–944.

Mayor, S., Rothberg, K.G., and Maxfield, F.R. (1994). Sequestration of GPI-anchored proteins in caveolae triggered by cross-linking. Science *264*, 1948–1951.

Mays, R.W., Siemers, K.A., Fritz, B.A., Lowe, A.W., van Meer, G., and Nelson, W.J. (1995). Hierarchy of mechanisms involved in generating Na/K-ATPase polarity in MDCK epithelial cells. J. Cell Biol. *130*, 1105–1115.

Montesano, R., Roth, J., Robert, A., and Orci, L. (1982). Non-coated membrane invaginations are involved in binding and internalization of cholera and tetanus toxins. Nature *296*, 651–653.

Nagy, P., Vamosi, G., Bodnar, A., Lockett, S.J., and Szollosi, J. (1998). Intensity-based energy transfer measurements in digital imaging microscopy. Eur. Biophys. J. *27*, 377–389.

Ng, T., *et al*. (1999). Imaging protein kinase Cα activation in living cells. Science *283*, 2085–2089.

Orlandi, P.A., and Fishman, P.H. (1998). Filipin-dependent inhibition of cholera toxin—evidence for toxin internalization and activation through caveolae-like domains. J. Cell Biol. *141*, 905–915.

Parton, R.G. (1994). Ultrastructural localization of gangliosides; GM1 is concentrated in caveolae. J. Histochem. Cytochem. *42*, 155–166.

Parton, R.G. (1996). Caveolae and caveolins. Curr. Opin. Cell Biol. *8*, 542–548.

Parton, R.G., Joggerst, B., and Simons, K. (1994). Regulated internalization of caveolae. J. Cell Biol. *127*, 1199–1215.

Pollok, B.A., and Heim, R. (1999). Using GFP in FRET-based applications. Trends Cell Biol. *9*, 57–60.

Rothberg, K.G., Ying, Y.S., Kamen, B.A., and Anderson, R.G. (1990). Cholesterol controls the clustering of the glycophospholipid-anchored membrane receptor for 5-methyltetrahydrofolate. J. Cell Biol. *111*, 2931–2938.

Sargiacomo, M., Sudol, M., Tang, Z., and Lisanti, M.P. (1993). Signal transducing molecules and glycosyl-phosphatidylinositol-linked proteins form a caveolin-rich insoluble complex in MDCK cells. J. Cell Biol. *122*, 789–807.

Schnitzer, J.E., Oh, P., and McIntosh, D.P. (1996). Role of GTP hydrolysis in fission of caveolae directly from plasma membranes. Science *274*, 239–242.

Sheets, E.D., Lee, G.M., Simson, R., and Jacobson, K. (1997). Transient confinement of a glycosylphosphatidylinositol-anchored protein in the plasma membrane. Biochemistry *36*, 12449–12458.

Siddle, K., Bailyes, E.M., and Luzio, J.P. (1981). A monoclonal antibody inhibiting rat liver 5′ nucleotidase. FEBS Lett. *128*, 103–107.

Simons, K., and Ikonen, E. (1997). Functional rafts in cell membranes. Nature *387*, 569–572.

Simons, M., Friedrichson, T., Schulz, J.B., Pitto, M., Masserini, M., and Kurzchalia, T.V. (1999). Exogenous administration of gangliosides displaces GPI-anchored proteins from lipid microdomains in living cells. Mol. Biol. Cell *10*, 3187–3196.

Skibbens, J.E., Roth, M.G., and Matlin, K.S. (1989). Differential extractability of influenza hemagglutinin during intracellular transport in polarized epithelial cells and nonpolar fibroblasts. J. Cell Biol. *108*, 821–832.

Smart, E.J., Mineo, C., and Anderson, R.G. (1996). Clustered folate receptors deliver 5-methyltetrahydrofolate to cytoplasm of MA104 cells. J. Cell Biol. *134*, 1169–1177.

Smart, E.J., Ying, Y.S., Mineo, C., and Anderson, R.G.W. (1995). A detergent-free method for purifying caveolae membrane from tissue culture cells. Proc. Natl. Acad. Sci. USA *92*, 10104–10108.

Stauffer, T.P., and Meyer, T. (1997). Compartmentalized IgE receptor-mediated signal transduction in living cells. J. Cell Biol. *139*, 1447–1454.

Stefanova, I., Hilgert, I., Kristofova, H., Brown, R., Low, M.G., and Horejsi, V. (1989). Characterization of a broadly expressed human leukocyte antigen MEM43 anchored in membrane through phosphatidylinositol. Mol. Immunol. *26*, 153–161.

Stefanova, I., Horejsi, V., Ansotegui, I.J., Knapp, W., and Stockinger, H. (1991). GPI-anchored cell-surface molecules complexed to protein tyrosine kinases. Science *254*, 1016–1019.

Strohmeier, G.R., Lencer, W.I., Pataposs, T.W., Thompson, L.F., Carson, S.L., Moe, S.J., Carnes, D.K., Mrsny, R.J., and Madara, J.L. (1997). Surface expression, polarization, and functional significance of CD73 in human intestinal epithelia. J. Clin. Invest. *99*, 2588–2601.

Tsien, R.Y., Bacskai, B.J., and Adams, S.R.. (1993). FRET for studying intracellular signaling. Trends Cell Biol. *3*, 242–245.

Uster, P.S., and Pagano, R.E. (1986). Resonance energy transfer microscopy: observations of membrane-bound fluorescent probes in model membranes and in living cells. J. Cell Biol. *103*, 1221–1234.

van den Berg, C.W., Cinek, T., Hallett, M.B., Horejsi, V., and Morgan, B.P. (1995). Exogenous glycosyl phosphatidylinositol-anchored

CD59 associates with kinases in membrane clusters on U937 cells and becomes Ca2+-signaling competent. J. Cell Biol. *131*, 669–677.

Varma, R., and Mayor, S. (1998). GPI-anchored proteins are organized in submicron domains at the cell surface. Nature *394*, 798–801.

Verkade, P., and Simons, K. (1997). Lipid microdomains and membrane trafficking in mammalian cells. Histochem. Cell Biol. *108*, 211–220.

Walsh, L.A., Trone, M., Thiru, S., and Walsmann, H. (1992). The CD59 antigen—a multifunctional molecule. Tissue Antigens *40*, 213–220.

Weimbs, T., Low, S.H., Chapin, S.J., and Mostov, K.E. (1997). Apical targeting in polarized epithelial cells—there's more afloat than rafts. Trends Cell Biol. *7*, 393–399.

Wolber, P.K., and Hudson, B.S. (1979). An analytic solution to the Förster energy transfer problem in two dimensions. Biophys. J. *28*, 197–210.

Wolf, A.A., Jobling, M.G., Wimer-Mackin, S., Ferguson-Maltzman, M., Madara, J.L., Holmes, R.K., and Lencer, W.I. (1998). Ganglioside structure dictates signal transduction by cholera toxin and association with caveolae-like membrane domains in polarized epithelia. J. Cell Biol. *141*, 917–927.

Wu, M., Fan, J., Gunning, W., and Ratnam, M. (1997). Clustering of GPI-anchored folate receptor independent of both cross-linking and association with caveolin. J. Membr. Biol. *159*, 137–147.

Zimmermann, H. (1992). 5′-Nucleotidase: molecular structure and functional aspects. Biochem. J. *285*, 345–365.